

STUDY OF METHYLENE BLUE PHOTODYNAMIC ACTIVITY ON ERYTHROCYTE SUSPENSIONS IN VITRO

Markova I.V.^{1,2}, Ryabova A.V.^{1,2}, Romanishkin I.D.¹, Pominova D.V.^{1,2}

¹Prokhorov General Physics Institute of Russian Academy of Sciences, Moscow, Russia

²National Research Nuclear University MEPhI (Moscow Engineering Physics Institute), Moscow, Russia

Abstract

In this paper we studied the photodynamic activity (the rate of molecular oxygen utilization during irradiation) of methylene blue (MB) in erythrocyte suspensions in vitro. Using spectroscopy and confocal microscopy with fluorescent sensors for singlet oxygen and other active oxygen species, it was shown that with an increase in the MB concentration (10–100 mg/kg), the molar photodynamic activity decreases. It was found that 5–10% of the MB added to erythrocytes tightly binds to the erythrocyte membranes, and the generation of singlet oxygen ($^{1}O_{2}$) is suppressed in favor of type I reactions (formation of $H_{2}O_{2}$, O_{2} , * , * OH). Another 40% of the MB added to erythrocytes is converted into a colorless leuco form, but is reoxidized back to MB under photodynamic exposure. The maximum relative quantum yield of $^{1}O_{2}$ generation (ϕ_{Δ}) among those measured in erythrocyte suspensions was 0.014 for a 10 mg/kg MB concentration, which is an order of magnitude lower than the values for MB in organic solvents and for the aluminum sulfonated phthalocyanine comparison photosensitizer (PS) (ϕ_{Δ} = 0.38). Interaction with erythrocytes (aggregation, reduction to the leuco form, competition for oxygen) explains the decrease in the MB efficiency under physiological conditions compared to organic solvents. The obtained results are important from the point of view of optimizing the systemic use of MB in photodynamic therapy.

Keywords: methylene blue, spectroscopy, absorption, fluorescence, photobleaching, ROS, singlet oxygen.

Contacts: Pominova D.V., e-mail: pominovadv@gmail.com

For citations: Markova I.V., Ryabova A.V., Romanishkin I.D., Pominova D.V. Study of methylene blue photodynamic activity on erythrocyte suspensions *in vitro*, *Biomedical Photonics*, 2025, vol. 14, no. 3, pp. 4–13. doi: 10.24931/2413–9432–2025–14–3–4–13

ИССЛЕДОВАНИЕ ФОТОДИНАМИЧЕСКОЙ АКТИВНОСТИ МЕТИЛЕНОВОГО СИНЕГО НА СУСПЕНЗИЯХ ЭРИТРОЦИТОВ IN VITRO

И.В.Маркова 1,2 , А.В. Рябова 1,2 , И.Д.Романишкин 1 , Д.В. Поминова 1,2

¹Институт общей физики им. А. М. Прохорова Российской академии наук, Москва, Россия ²Национальный исследовательский ядерный университет «МИФИ», Москва, Россия

Резюме

В работе исследована фотодинамическая активность (по скорости утилизации молекулярного кислорода при облучении) метиленового синего (МС) в суспензиях эритроцитов *in vitro*. Методами спектроскопии и конфокальной микроскопии с флуоресцентными сенсорами на синглетный кислород и другие активные формы кислорода показано, что при увеличении концентрации МС (10-100 мг/кг) молярная фотодинамическая активность снижается. Установлено, что 5-10% от добавленного к эритроцитам МС прочно связывается с мембранами эритроцитов, а генерация синглетного кислорода ($^{1}O_{2}$) подавляется в пользу реакций I типа (образование $H_{2}O_{2}$, O_{2} , $^{-}$, $^{-}$ OH). Еще порядка 40% от добавленного к эритроцитам МС переходит в бесцеетную лейкоформу, однако при фотодинамическом воздействии окисляется обратно до МС. Максимальный квантовый выход генерации $^{1}O_{2}$ (ϕ_{Δ}) в суспензиях эритроцитов составил 0,014 для концентрации МС 10 мг/кг, что на порядок ниже значений для МС в органических растворителях и для фотосенсибилизатора сравнения фотосенс ($\phi_{\Delta} = 0,38$). Взаимодействие с эритроцитами (агрегация, восстановление в лейкоформу, конкуренция за кислород) объясняет снижение эфективности МС в физиологических условиях по сравнению с органическими растворителями. Полученные результаты важны с точки зрения оптимизации системного применения МС в фотодинамической терапии.

Ключевые слова: метиленовый синий, спектроскопия, поглощение, флуоресценция, фотообесцвечивание, АФК, синглетный кислород.

Контакты: Поминова Д.В., e-mail: pominovadv@gmail.com

Для цитирования: Маркова И.В., Рябова А.В., Романишкин И.Д., Поминова Д.В. Исследование фотодинамической активности метиленового синего на суспензиях эритроцитов *in vitro* // Biomedical Photonics. – 2025. – Т. 14, № 3. – С. 4–13. doi: 10.24931/2413–9432–2025–14–3–4–13

Introduction

Photodynamic Therapy (PDT) is a method based on the interaction of a photosensitizer (PS), light of a specific wavelength, and molecular oxygen (3O_2). The interaction of these components results in the formation of cytotoxic reactive oxygen species (ROS). Upon light irradiation, the PS transition from its ground state to an excited singlet state occurs, followed by intersystem conversion to a triplet state. Depending on the ROS generation mechanism, two types of reactions are distinguished: Type I – hydrogen removal or electron transfer between the PS excited triplet state and a substrate, leading to the formation of free radicals (H_2O_2 , •OH, O_2 •-); Type II – energy transfer from the PS triplet state to molecular oxygen, generating highly reactive singlet oxygen (1O_2) [1, 2].

Singlet oxygen generation results in a potent cytotoxic effect and is a more efficient mechanism of photodynamic action. However, although the Type II mechanism is considered dominant in most PDT scenarios, Type I becomes more relevant under the hypoxic conditions, characteristic for tumor tissues [3, 4]. The cytotoxic ROS generated by Type I photodynamic reactions, including H_2O_2 , •OH, and O_2 •¯, can stimulate cell apoptosis or necrosis, vascular damage, and immune system activation [5, 6]. PDT is currently widely used in clinical practice [7–12].

The ratio between Type I and Type II reactions depends on the photophysical properties of the chosen PS. Methylene blue (MB), a cationic thiazine dye, is extensively studied as a PS. MB has been used effectively for PDT of various tumors [13]. According to the literature, MB can generate singlet oxygen with a high quantum yield ($\phi\Delta$ ~0.5 in CH₃OH, 0.52 in EtOH), which, combined with relatively low dark toxicity [14, 15], makes it an attractive PS. However, it should be noted that measurements of singlet oxygen quantum yield are primarily performed in ethanol or organic solvents [15].

Currently, the clinical application of MB is limited by several factors related to its aggregation in aqueous environments and interactions with biological systems, such as erythrocytes. In aqueous solutions at concentrations about 10 µM, MB tends to aggregate, forming dimers, trimers, and higher-order aggregates [16, 17]. Aggregate formation alters absorption and fluorescence spectra, fluorescence lifetime, and the photophysical characteristics of the dye, thereby affecting its photodynamic activity and efficacy as a PS [5, 18]. MB forms H-aggregates, whose fluorescence intensity is lower than that of monomers; consequently, luminescence intensity decreases as the dimer/ monomer ratio increases. A strong correlation has been demonstrated between changes in photophysical properties and solvent polarity, viscosity, and dielectric constant. The critical concentration for MB aggregation is higher in solvents with a greater dielectric constant, and MB aggregation in alcohols differs from that in

aqueous solutions, highlighting the importance of the solvent environment for studies of MB aggregation and photophysical properties in medical applications [17]. Data indicate that MB aggregation and dimerization also alter the type of photodynamic reaction [18]; MB dimers predominantly undergo electron transfer pathways to deactivate the excited state (Type I reaction), with almost complete suppression of singlet oxygen generation [19].

Beyond concentration-dependent aggregation, the positively charged MB can bind to negatively charged cell membranes [19, 20]. The interaction of MB with erythrocytes has been actively investigated in the context of treating methemoglobinemia - a condition caused by oxidative stress where hemoglobin is oxidized to methemoglobin (MetHb), losing its oxygen-carrying capacity [21]. Upon interaction with erythrocytes, MB accumulates within them via a "reductive uptake" mechanism: upon entering the cell, it is reduced by NADPH-dependent enzymes of the pentose phosphate pathway to colorless leuco-methylene blue (LMB), which does not absorb light in the red region, loses its photosensitizing ability, and is retained intracellularly until re-oxidation occurs [22]. During methemoglobinemia, MB within erythrocytes acts as a cofactor for the flavin reductase enzyme (biliverdin reductase B, BLVRB), accelerating the reduction of MetHb to functional hemoglobin: oxidized MB (blue) accepts electrons from NADPH via BLVRB, converting to LMB. LMB directly reduces MetHb, itself being oxidized back to MB and closing the catalytic cycle [21, 23– 26]. This process can limit the photodynamically effective concentration of MB after its systemic administration.

MB enhances the respiratory metabolism of erythrocytes, increasing O_2 consumption, which may lead to hypoxia in the irradiation zone [27]. However, in the case of tumors, systemic administration in vivo may conversely increase oxygenation over time due to a metabolic shift towards oxidative phosphorylation [28, 29].

Thus, numerous factors influence the photodynamic activity of MB. Although the interaction of MB with erythrocytes has been well studied in the context of methemoglobinemia treatment, the impact of this interaction on MB's photodynamic activity has not been studied. Under physiological conditions, MB's behavior fundamentally differs from that in organic solvents and alcohols: interaction with erythrocytes, reduction to the leuco-form, and competition for oxygen radically alter its photophysical properties upon systemic administration.

In this work, we investigated the photodynamic activity of MB in erythrocyte suspensions, assessing the influence of dimerization, reduction to LMB, and interaction with erythrocytes on the type of photodynamic reaction (I or II). The results will enable optimization of PDT parameters for systemic MB administration, explain the limitations of its clinical application, and propose strategies to overcome these limitations.



Materials and methods

Sample Preparation

An erythrocyte suspension was prepared in saline (40% red blood cells, 60% saline). The suspension pH was maintained at physiological level. The erythrocyte suspension was then mixed with the investigated PS in a 1.5 ml Eppendorf tube and incubated at 37°C in complete darkness. A 1% aqueous solution of MB (JSC "Samaramedprom", Russia) was used. The investigated MB concentrations were 0, 1, 10, 20, 40, 60, 80, and 100 mg/kg. For comparison, the aluminum sulfonated phthalocyanine-based PS photosens® (NIOPIK, Russia) was used at a concentration of 1 mg/kg; its singlet oxygen quantum yield is reported to be 0.38.

Detection of ROS and Singlet Oxygen Using Fluorescent Indicators

The fluorescent indicator 6-carboxy-2',7'-dichlorodihydrofluorescein diacetate (c-H₂DCFDA, Lumiprobe, Russia) at 25 µM was used to assess ROS generation (H₂O₂, O₂•-, •OH, ROOH, ONOO-). Singlet Oxygen Sensor Green (SOSG, Lumiprobe, Russia) at 10-100 µM was used to detect singlet oxygen (¹O₂) in aqueous solutions. The erythrocyte suspension was incubated with MB (0-100 mg/kg) in saline for 30 min at 37°C. The fluorescent indicator was then added, followed by another 30 min incubation. To generate ROS, samples were irradiated with a laser (660 nm, 40 mW/cm², dose 50 J/cm²). Fluorescence of the ROS indicators (c-H₂DCFDA and SOSG) was recorded using an inverted confocal microscope LSM-710-NLO (Carl Zeiss, Germany) with 488 nm excitation and detection in the 510-580 nm range. Additionally, PS fluorescence was recorded using 633 nm laser excitation and signal detection in the 650-730 nm range. Fluorescence intensities of the indicators and PS were analyzed, averaged over the image.

Spectrophotometric Analysis of MB Aggregation and Binding to Erythrocytes

Incubation of PS with erythrocyte suspensions was performed for 15 min, after which absorption spectra were measured. To evaluate MB binding to erythrocytes, samples were centrifuged for 5 min at 3570 g, the supernatant was removed and replaced with fresh saline (this procedure was repeated twice), and measurements were repeated.

Absorption spectra were recorded using a Hitachi U3400 spectrophotometer (Japan) in quartz cuvettes (1 mm optical path) over the 200-1000 nm range. To analyze MB aggregation and binding to erythrocytes, the spectra were approximated by the sum of three spectra corresponding to erythrocyte absorption, MB absorption at 10 mg/kg, and background signal (scattering). The shape of the experimental spectrum and the approximation were compared, and differences were analyzed. Since the shape of the MB absorption spectrum depends on concentration, the form of the MB

absorption spectrum was determined by subtracting the approximated erythrocyte absorption spectra and background from the experimentally recorded absorption spectra of erythrocyte suspensions containing MB.

Evaluation of MB Photodynamic Activity and Singlet Oxygen Generation Efficiency by Spectroscopic Methods

The photodynamic activity of MB was assessed spectroscopically by the rate of hemoglobin deoxygenation during PDT [30, 31] with PS (MB or aluminum sulfonated phthalocyanine) on erythrocyte suspensions.

Samples consisted of an erythrocyte suspension with PS in saline, were placed between two coverslips separated by a 200 µm thick plastic spacer. The sample volume was 100 μl. Hemoglobin oxygenation was evaluated based on absorption spectra measured using a LESA-01-Biospec spectrophotometer (Biospec, Russia) with a halogen lamp light source. This was done by approximating the measured absorption spectrum as the sum of the absorption spectra of oxygenated hemoglobin, deoxygenated hemoglobin, and background scattering (linear dependence). Hemoglobin oxygenation was calculated as the ratio of oxygenated hemoglobin absorption to the total (oxyand deoxy-) hemoglobin absorption. For PDT, samples were irradiated within the PS absorption band using a semiconductor laser source (wavelength 660 nm, power density 167 mW/cm²; irradiation duration 8 min). The experimental setup is shown in Fig. 1.

During PDT mediated by a Type II PS, the generated $^{1}O_{2}$ undergoes irreversible reactions with biological molecules, leading to a decrease in dissolved $^{3}O_{2}$ in the sample and, consequently, hemoglobin deoxygenation. Thus, the photodynamic activity of the investigated PS can be evaluated by the rate of hemoglobin deoxygenation.

The relative quantum yield of 1O_2 generation ($\varphi\Delta$) can be quantitatively assessed to evaluate PS efficiency. This requires comparing the hemoglobin deoxygenation rate using the investigated PS with the rate using a PS of known quantum yield. The relative quantum yield of 1O_2 generation for MB concentrations of 10-100 mg/kg can then be calculated using the relationship:

$$\varphi_{\Delta}(MB) = \frac{C(PS) \cdot \tau(PS)}{C(MB) \cdot \tau(MB)} \cdot \varphi_{\Delta}(PS) \tag{1}$$

where C is concentration and τ is deoxygenation time. The τ value was determined from experimentally measured deoxygenation curves using the doseresponse relationship:

$$f(t) = \max -\frac{max - min}{1 + \left(\frac{t}{\tau}\right)^{min}},$$
 (2)

where *t* is time, *max* is the maximum asymptote value, *min* is the minimum asymptote value (Fig. 2).

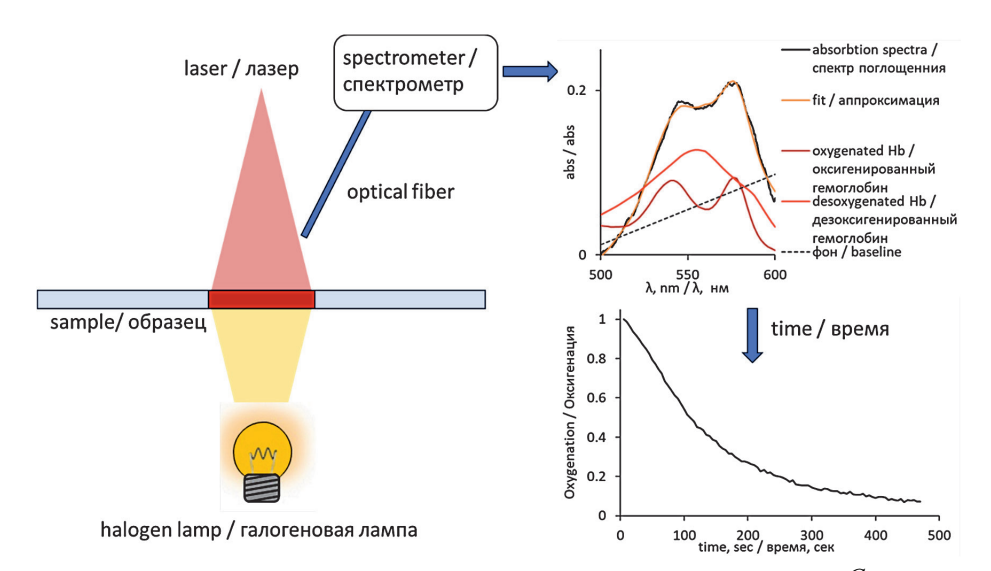


Рис. 1. Схема установки для измерения скорости дезоксигенации гемоглобина.

Fig. 1. Schematic representation of the setup for hemoglobin deoxygenation rate measuring.

The difference between the maximum and minimum asymptotes (delta, the change in oxygenation value over a measured time interval) and the steepness of the curve slope (deoxygenation rate) were also determined from the dependence.

In addition to the relative quantum yield, the photodynamic activity of MB was calculated as a quantitative characteristic of $^{1}O_{2}$ generation efficiency. It is known that during PDT, if oxygen deficiency is not a limiting factor and under low irradiance where ground state PS depletion is negligible, the oxygen consumption rate is expressed by the following equation:

$$\Gamma_{PDT} = \alpha \cdot \varphi_{ch} \cdot C \cdot P, \tag{3}$$

where Γ_{PDT} is the oxygen consumption rate, M/(l·s); α is the singlet oxygen generation efficiency coefficient, cm²/J; φ_{ch} is the quantum yield of chemical (irreversible) quenching of 1O_2 ; C is the molar concentration of PS, M; P is the irradiance, W/cm². The singlet oxygen generation efficiency coefficient (i.e., the number of 1O_2 molecules generated per PS molecule per light dose of 1 J/cm²) is calculated by:

$$\alpha = \frac{\sigma}{E_{loc}} \cdot \varphi_{\Delta} \approx 1.923 \times 10^{-5} \cdot \varepsilon \cdot \lambda \cdot \varphi_{\Delta}, \tag{4}$$

where $\sigma = \frac{ln10 \cdot \varepsilon}{N_{\scriptscriptstyle A}} -$ absorption cross-section of the PS

molecule, cm²; $E_{hv} = \frac{h \cdot c}{\lambda}$ – photon energy, J; ϕ_{Δ} – quantum

yield of $^{1}O_{2}$ formation; λ – irradiation wavelength, nm; ε – extinction coefficient of the PS, L·mol $^{-1}$ ·cm $^{-1}$. We used extinction coefficient values ε in saline at λ =660 nm: for MB 53300 L·mol $^{-1}$ ·cm $^{-1}$ [32], for aluminum sulfo-nated phthalocyanine 82000 L·mol $^{-1}$ ·cm $^{-1}$.

The PDT oxygen consumption rate $\Gamma_{_{PDT}}$ can also be experimentally estimated from the change in hemoglobin oxygen saturation in the sample:

$$\Gamma_{PDT} = -4 \cdot \left[Hb_{tot} \right] \cdot \frac{dS_{O_2}}{dt},\tag{5}$$

where $[Hb_{tot}] = \frac{C_{Hb}}{M_{Hb}}$ – total molar concentration of hemoglobin tetramer in the sample, mol/L; $\frac{dS_{O_2}}{dt}$ – rate

of change of hemoglobin oxygen saturation; C_{Hb} – hemoglobin concentration in blood (typically 130-150 g/L, in our case 152 g/L), g/L; M_{-Hb} = 66,500 g/mol – molecular weight of the hemoglobin molecule (tetramer).

Due to the low probability of chemical quenching of $^1\text{O}_2$ molecules, it is more convenient to evaluate the photodynamic activity Ψ as the probability of chemical quenching of a $^1\text{O}_2$ molecule per 100 photons absorbed by the PS: $\Psi = \varphi_{\scriptscriptstyle \Lambda} \cdot \varphi_{\scriptscriptstyle ch} \cdot 100. \tag{6}$

Using equations (3 – 5) and substituting the value of $\phi_{_ch'}$ we obtain from the slope of the experimental hemoglobin deoxygenation curve at the initial time point after PDT onset:

$$\Psi = 5.2 \times 10^{6} \cdot \frac{-4 \left[Hb_{tot} \right] \cdot \frac{dS_{O_{2}}}{dt}}{\lambda \cdot \varepsilon \cdot C \cdot P}, \tag{7}$$

where $\frac{dS_{O_2}(0)}{dt} = \frac{S_{O_2}(0)}{\tau}$ – rate of change of hemoglobin

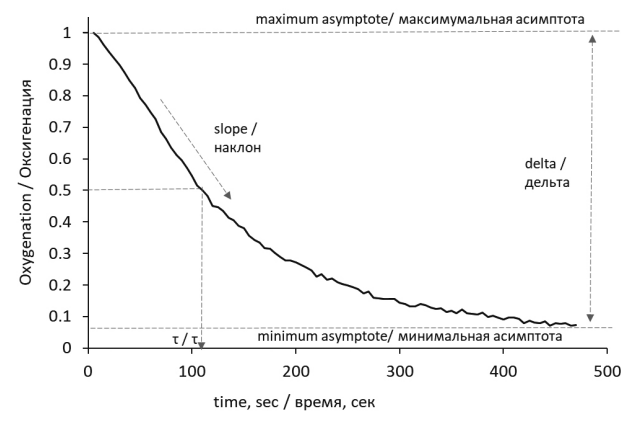


Рис. 2. Зависимость «доза-ответная реакция» и ее основные параметры.

Fig. 2. Dose-response function and its main parameters.



oxygen saturation at the initial moment of irradiation. Substituting PS molar concentrations in μ M, wavelength 660 nm, irradiance 167 mW/cm², and an initial hemoglobin oxygenation level of 0.7 for our samples, we obtain the resulting formula for calculating the photodynamic activity of MB:

$$\Psi = 3.02 \times 10^8 \cdot \frac{1}{\varepsilon \cdot C \cdot \tau}.$$
 (8)

All measurements were performed in triplicate and then averaged. Data are presented as mean \pm standard deviation. Groups were compared using Student's t-test (p < 0.05 considered significant).

Results and discussion

Investigation of Methylene Blue Photodynamic Activity Using Fluorescent Indicators

Results of studying the photodynamic activity of MB and aluminum sulfonated phthalocyanine using fluorescent indicators – SOSG for detecting singlet oxygen ($^{1}O_{2}$) and c-H $_{2}$ DCFDA for detecting ROS other than singlet oxygen ($^{1}O_{2}$) o $_{2}$. •OH) – revealed that irradiation of erythrocyte suspensions with aluminum sulfonated phthalocyanine resulted in increased SOSG fluorescence intensity compared to the control, indicating singlet oxygen generation. The fluorescence intensity of aluminum sulfonated phthalocyanine increased with increasing irradiation dose, Fig. 3.

After 10 min of irradiation, SOSG fluorescence intensity decreased due to erythrocyte lysis and quenching of the indicator's fluorescence by hemoglobin. SOSG fluorescence intensity after irradiation of erythrocyte suspensions with MB was significantly lower than with aluminum sulfonated phthalocyanine and remained unchanged with increasing irradiation dose. It is also noteworthy that at the same irradiation dose, SOSG fluorescence intensity slightly decreased with increasing MB concentration, suggesting suppression of ¹O₂ generation associated with MB aggregation.

The fluorescence intensity of the PS itself as a function of irradiation dose was also assessed, Fig. 4.

The fluorescence intensity of aluminum sulfonated phthalocyanine and MB showed no significant change

with irradiation dose. Probable explanations include dissociation of MB dimers at low doses, followed by photobleaching and conversion of MB to LMB in an oxygen-depleted environment.

When studying erythrocyte suspensions with c-H₂DCFDA and MB, an increase in indicator fluorescence intensity was observed with increasing MB concentration, indicating the role of MB aggregation in shifting towards Type I reactions and ROS generation, Fig. 5.

Interestingly, an increase in c-H₂DCFDA fluorescence intensity after irradiation was observed for both MB and aluminum sulfonated phthalocyanine, the latter being a Type II PS primarily generating singlet oxygen. Although ¹O₂ poorly oxidizes c-H₂DCFDA to its fluorescent form directly, several indirect mechanisms may explain this phenomenon in erythrocyte suspensions [33–36]. Firstly, indirect oxidation of c-H₂DCFDA via secondary ROS is possible. Reactions of ¹O₂ or radicals formed during its interaction can lead to hydrogen peroxide (H₂O₂) formation and increased c-H₂DCFDA fluorescence. The influence of this mechanism is supported by studies in physiological saline without erythrocytes (Fig. 5), where an increase in c-H₂DCFDA fluorescence after irradiation was also observed.

In erythrocyte suspensions with aluminum sulfonated phthalocyanine, the c-H₂DCFDA signal increase was more pronounced compared to physiological saline, likely due to additional indirect oxidation via products of ¹O₂ reactions with cellular components. Singlet oxygen is highly reactive with double bonds in erythrocyte membrane lipids, leading to lipid hydroperoxide (LOOH) formation. Singlet oxygen can also damage heme, releasing iron, a potent catalyst for Fenton/Haber-Weiss reactions generating ROS. Methemoglobin (MetHb, Fe³⁺) or heme itself can decompose LOOH or H₂O₂ (formed from other ROS), generating highly reactive radicals (LO•, •OH) that oxidize c-H2DCFDA. Fe²⁺ ions also catalyze LOOH decomposition via the Fenton reaction:

$$LOOH + Fe^{2+} \rightarrow LO^{-} + OH^{-} + Fe^{3+},$$
 (9)

producing lipid alkoxyl radicals (LO•) that oxidize c-H₂DCFDA and initiate lipid peroxidation chain reactions,

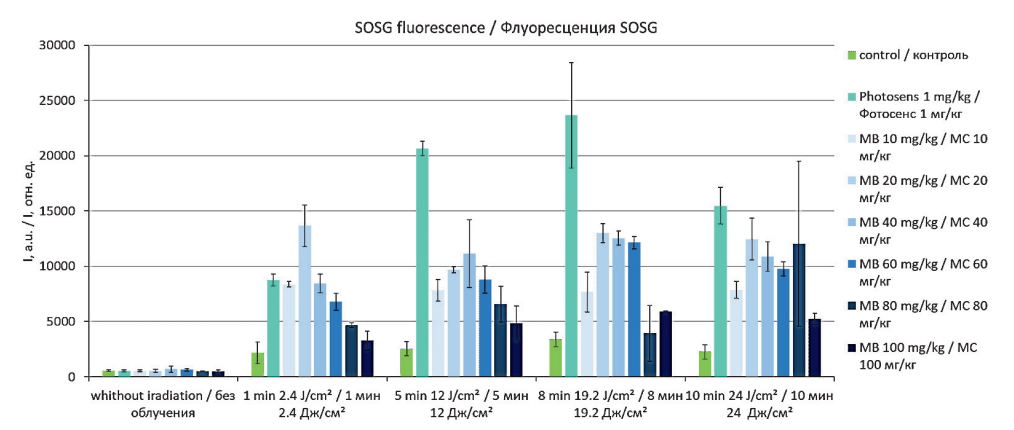


Рис. 3. Зависимость интенсивности флуоресценции индикатора SOSG для выявления синглетного кислорода от дозы облучения при различных концентрациях ФС.

Fig. 3. Dependence of the indicator for detecting singlet oxygen SOSG fluorescence intensity on the radiation dose at different concentrations of PS.

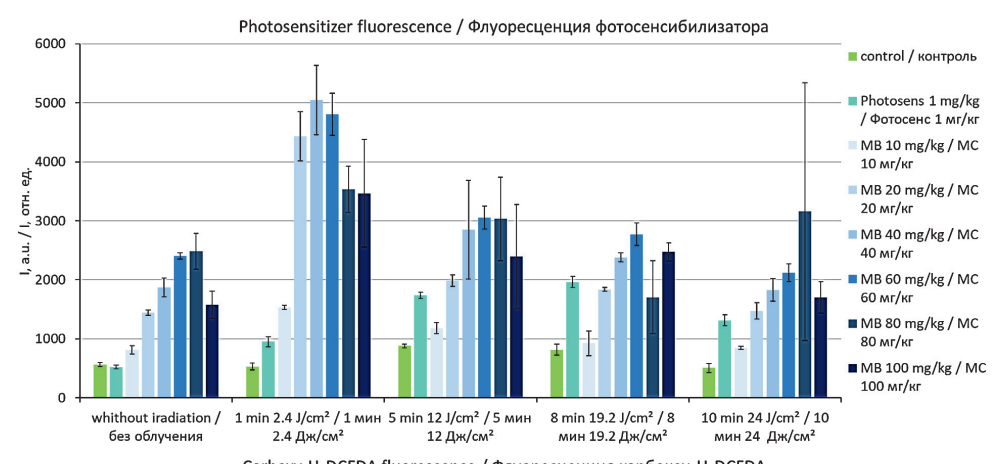




Fig. 4. Dependence of the studied PS fluorescence intensity on the irradiation dose at different concentrations of PS.

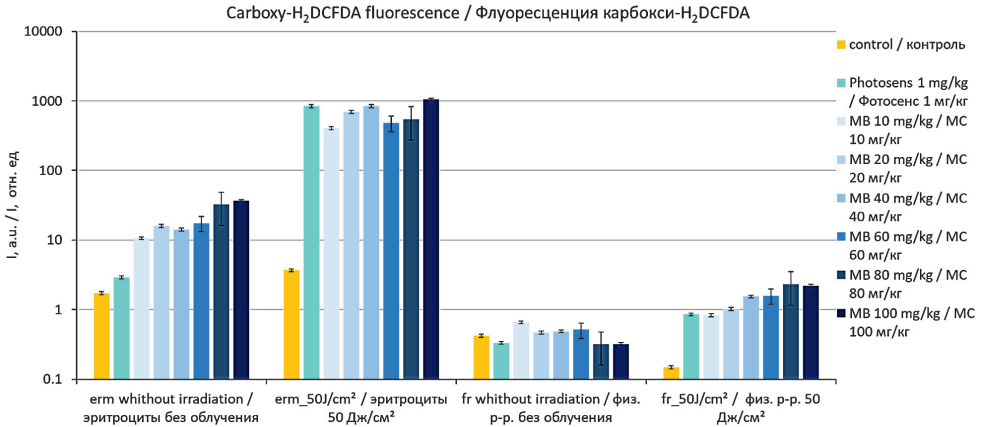


Рис. 5. Зависимость интенсивности флуоресценции индикатора с-H₂DCFDA для выявления АФК, отличных от синглетного кислорода. от дозы облучения при различных концентрациях ФС. Fig. 5. Dependence of the indicator for detecting ROS other than singlet oxygen c-HaDCFDA fluorescence intensity on the irradiation dose at different concentrations of PS.

generating new radicals (L•, LOO•) and peroxides, which can also oxidize c-H₂DCFDA.

эритроциты без облучения

Thus, c-H₂DCFDA fluorescence after irradiating erythro-cyte suspensions with a PS is a direct consequence of potent ¹O₂ generation within the lipid-rich, catalystabundant erythrocyte environment. 102 triggers a cascade of secondary reactions, and c-H₂DCFDA detects not the primary ¹O₂ itself, but the total oxidative stress arising from its reaction with key erythrocyte components and subsequent chain reactions catalyzed by hemoglobin and iron. The role of erythrocyte interaction is confirmed by the increased c-H₂DCFDA signal in control erythrocyte suspensions without added PS compared to physiological

When interpreting these results, it is important to consider sensor limitations. SOSG is relatively specific to ${}^{1}O_{2}$ but can react with other oxidants. c-H2DCFDA is oxidized by a broad spectrum of ROS and is non-specific. Moreover, hemoglobin itself can influence indicator fluorescence (absorption quenching) or conversely catalyze their oxidation. However, the contrast between the SOSG fluorescence data (aluminum sulfonated phthalocyanine >> MB) and c-H₂DCFDA data (MB > aluminum sulfonated phthalocyanine) convincingly indicates the predominance of different photodynamic mechanisms: Type II for aluminum sulfonated phthalocyanine and a mixed I/ Il type with dominance of Type I for MB in this system. Spectroscopic methods without additional indicators

may provide more precise results and allow quantitative assessment of ${}^{1}O_{2}$ generation efficiency.

Spectral Analysis of MB Aggregation and Binding to **Erythrocytes**

To evaluate MB aggregation upon interaction with erythrocytes, absorption spectra were recorded and changes in their shape within the 600-700 nm region (corresponding to MB absorption) were analyzed. Absorption spectra recorded for erythrocyte suspensions with various MB concentrations and their approximation as the sum of erythrocyte suspension and MB solution spectra are presented in Fig. 6.

Increasing of MB concentration led to greater divergence between experimentally measured spectra and the approximation. To recover the true absorption spectrum shape corresponding to MB within the erythrocyte suspension, the approximated erythrocyte absorption spectra and background were subtracted from the experimental data. The resulting MB absorption spectra were compared with experimental absorption spectra of the supernatant after centrifuging the MBtreated erythrocyte suspension, Fig. 7.

The shape of the absorption spectrum obtained via decomposition and subtraction completely matched the supernatant absorption spectrum and the shape of the MB spectrum in physiological saline, indicating that no additional MB aggregation occurs upon interaction with erythrocytes.



To assess MB binding to erythrocytes, absorption spectra of erythrocyte suspensions were recorded after centrifugation and three additional washes to remove unbound MB, followed by approximation, Fig. 8.

The MB absorption spectra obtained via approximation show that after washing, the MB absorption peak (~664 nm) is still present in the erythrocyte suspension spectra. Approximately 5% of the initial MB concentration (~5 mg/kg for an initial concentration of 100 mg/kg) remained bound to the erythrocytes.

Thus, it can be concluded that while interaction with erythrocytes does not induce additional aggregation, a portion of MB binds to erythrocyte membranes via electrostatic interactions.

Hemoglobin Deoxygenation Kinetics

Deoxygenation curves recorded for erythrocyte suspensions with different MB concentrations are presented in Fig. 9.

During irradiation, the hemoglobin deoxygenation rate increased with MB concentration. Interestingly, the deoxygenation rate for the sample with an initial MB concentration of 100 mg/kg, after washing to remove

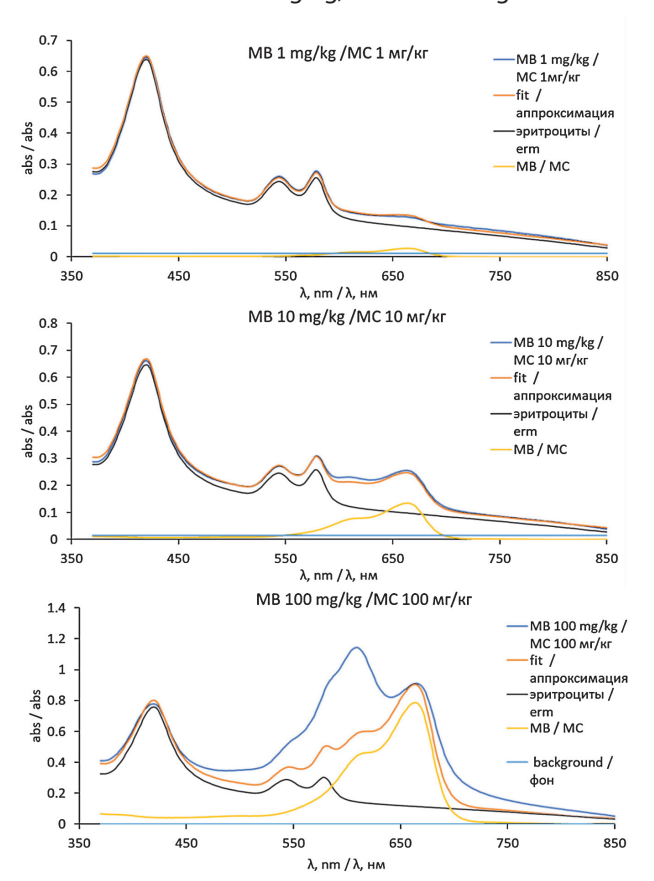


Рис. 6. Спектры поглощения, зарегистрированные для суспензии эритроцитов с концентрациями МС 1, 10 и 100 мг/кг, и их аппроксимация суммой спектров поглощения суспензии эритроцитов и раствора МС.

Fig. 6. Absorption spectra recorded for erythrocyte suspension with 1, 10 and 100 mg/kg MB and their approximation by the sum of the absorption spectra of the erythrocyte suspension and the MB solution.

unbound MB, corresponded to the rate observed at 60 mg/kg MB. This suggests that approximately 50% of the MB remained associated with the erythrocytes – ten times higher than the concentration determined spectrophotometrically. We hypothesize this discrepancy is due to the reduction of MB to LMB within erythrocytes. Erythrocytes possess potent reductive systems (NADPH and reduced glutathione, GSH) capable of reducing MB to LMB. Consequently, during pre-irradiation incubation with erythrocytes, a significant portion of MB may be converted intracellularly to the inactive leuco-form. MB primarily generates ROS via a Type I mechanism upon irradiation. These ROS attack and deplete key erythrocyte antioxidants. GSH is oxidized by radicals (especially •OH, HOCI, ONOO-) and peroxides. The enzyme glutathione peroxidase also consumes GSH to reduce H₂O₂ and lipid hydroperoxides. NADPH is critically required for glutathione reductase, which regenerates oxidized glutathione back to GSH. Under massive oxidative stress, NADPH and GSH reserves are rapidly depleted, diminishing the cell's reducing capacity and hindering the reduction of MB to LMB. Under these conditions, LMB can be oxidized back to MB by oxygen, ROS, or secondary oxidants

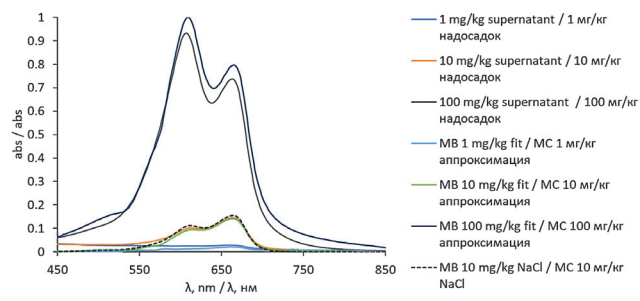


Рис. 7. Сравнение спектров поглощения МС, полученных в результате аппроксимации, с экспериментальными спектрами поглощения супернатанта после центрифугирования. Fig. 7. Comparison of the MB absorption spectra obtained as a result of approximation with the experimental absorption spectra of the supernatant after centrifugation.

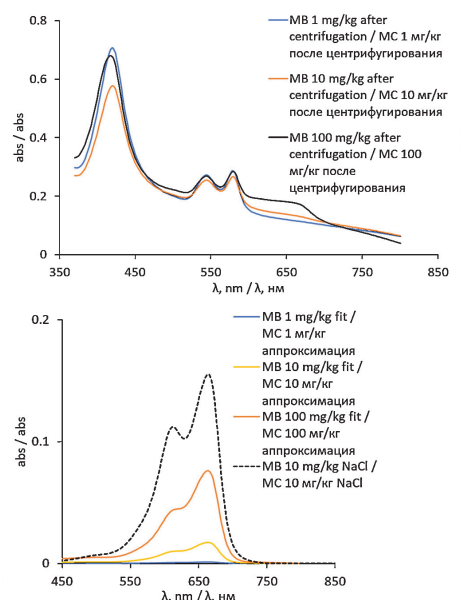


Рис. 8. Спектры поглошения эритроцитов после центрифугирования и дополнительной трехкратной отмывки от МС и спектры поглощения МС, полученные в результате аппроксимации. Fig. 8. Absorption spectra of erythrocytes after centrifugation and additional three-fold washing from MB and absorption spectra of MB obtained as a result of approximation.

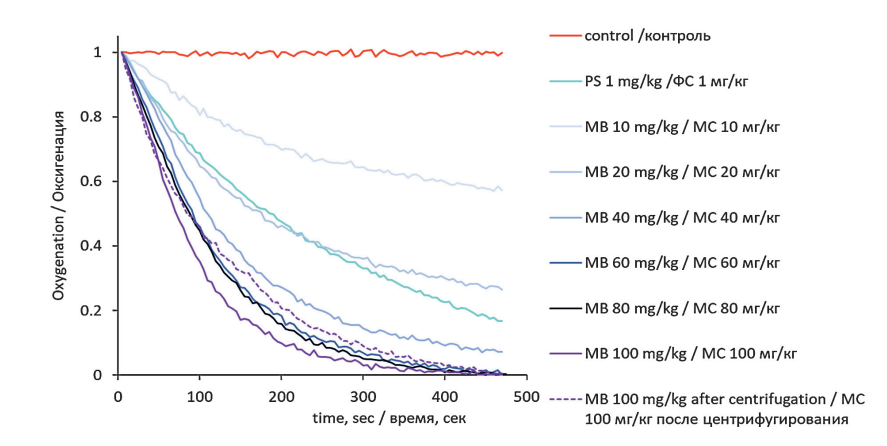


Рис. 9. Кривые дезоксигенации, зарегистрированные для суспензий эритроцитов с различной концентрацией MC. **Fig. 9.** Deoxygenation curves recorded for erythrocyte suspensions with different MB concentrations.

formed during antioxidant depletion. The oxidized MB can then generate new ROS upon further irradiation. Values obtained from deoxygenation curve fitting, along with calculated photodynamic activity (Ψ) and relative singlet oxygen quantum yield ($\varphi\Delta$) values, are presented in Table 1.

With increasing MB concentration, deoxygenation time decreased, while delta and the deoxygenation rate increased. This indicates that the amount of singlet oxygen generated increased with MB concentration. Deoxygenation time decreased from 33.8 sec (MB 10 mg/kg) to 15.8 sec (MB 100 mg/kg). However, photodynamic activity decreased with increasing MB concentration, Fig. 10.

Photodynamic activity represents the probability of chemical quenching of a ${}^{1}O_{2}$ molecule per 100 photons absorbed by the PS. The decrease in photodynamic activity with increasing MB concentration indicates that the number of photons absorbed by the PS grows faster than the number of singlet oxygen molecules generated. Over the concentration range studied, the efficiency of singlet oxygen generation was relatively low. The relative quantum yield of ${}^{1}O_{2}$ generation was 0.014 at 10 mg/kg MB and

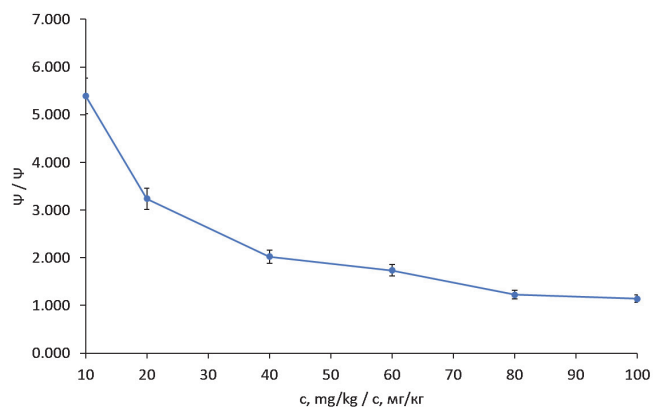


Рис. 10. Зависимость фотодинамической активности от концентрации MC.

Fig. 10. Dependence of photodynamic activity on the MB concentration.

0.003 at 100 mg/kg MB, one to two orders of magnitude lower than for aluminum sulfonated phthalocyanine ($\phi\Delta$ = 0.38), respectively. This supports the hypothesis that the photodynamic reaction for MB proceeds predominantly via Type I, generating ROS other than singlet oxygen.

Таблица 1

Полученные в результате аппроксимации кривых дезоксигенации значения времени дезоксигенации (τ), изменения значения оксигенации за измеренный промежуток времени (дельта), скорости дезоксигенации (наклон) и рассчитанные значения фотодинамической активности (Ψ) и относительного квантового выхода генерации синглетного кислорода ($\phi\Delta$)

Table 1

The values of deoxygenation time (τ) , change in oxygenation value over a measured time interval (delta), deoxygenation rate (slope), and calculated values of photodynamic activity (Ψ) and relative quantum yield of singlet oxygen generation $(\phi\Delta)$ obtained as a result of deoxygenation curve approximation

| | c, мг/кг c, mg/kg | c, мκM c, μM | τ, c τ, sec | дельта delta | наклон slope | Ψ | $\phi_{\scriptscriptstyle \Delta}$ |
|---|----------------------|-----------------|----------------|-----------------|-----------------|-------|------------------------------------|
| MC MB | 10 | 31 | 33.8 | 0.56 | 1.27 | 5.39 | 0.014 |
| | 20 | 63 | 27.7 | 0.9 | 1.26 | 3.24 | 0.008 |
| | 40 | 125 | 22.3 | 0.99 | 1.75 | 2.02 | 0.005 |
| | 60 | 188 | 17.3 | 1 | 1.96 | 1.74 | 0.004 |
| | 80 | 250 | 18.4 | 1 | 2.16 | 1.23 | 0.003 |
| | 100 | 313 | 15.8 | 1 | 2.27 | 1.14 | 0.003 |
| сульфированный фталоцианин алюминия sulfated aluminum phthalocyanine | 1 | 1 | 37.5 | 1 | 1.49 | 97.99 | 0.380 |



Thus, data obtained using fluorescent indicators and spectroscopy on MB-mediated ROS generation and the low quantum yield of singlet oxygen generation confirm the hypothesis of a shift in the photosensitization mechanism from Type II to Type I upon MB interaction with erythrocytes.

Conclusion

It has been established that the interaction of MB with erythrocytes radically alters its photophysical and photodynamic properties compared to those observed in organic solvents. A key finding is the significant suppression of singlet oxygen (102) generation – the relative quantum yield $(\phi\Delta)$ does not exceed 0.014 (at an MB concentration of 10 mg/ kg) and decreases to 0.003 at 100 mg/kg. This is 1-2 orders of magnitude lower than values characteristic of MB in alcohols $(\phi\Delta \sim 0.5)$ and the reference photosensitizer aluminum sulfonated phthalocyanine ($\phi\Delta$ = 0.38). This reduction is attributed to several interrelated factors: aggregation of MB molecules, their specific interaction with erythrocytes, and conversion to the inactive reduced form LMB.

It was experimentally confirmed that approximately 5% of the added MB binds to erythrocyte membranes via electrostatic interactions. Over 40% of MB is reduced to LMB by erythrocyte enzymes (NADPH-dependent

systems). However, under photodynamic action, LMB can be oxidized back to active MB, particularly against the backdrop of depletion of the cell's antioxidant reserves (NADPH, glutathione) induced by the generated ROS.

The combined use of fluorescent indicators (SOSG for ¹O₂ and c-H₂DCFDA for other ROS) and spectroscopic analysis of hemoglobin deoxygenation unequivocally demonstrates a shift in the mechanism of MB's photodynamic action in the presence of erythrocytes from Type II (dominant in organic media) towards Type I. This is manifested by enhanced generation of reactive oxygen species concurrent with suppressed ¹O₂ yield.

An important practical conclusion is the demonstration of an inverse relationship between the molar photodynamic activity (Ψ) of MB and its concentration within the studied range (10–100 mg/kg). Increasing the MB concentration does not overcome for the loss of efficacy associated with its interaction with the biological substrate and may even exacerbate it, likely due to enhanced aggregation and reduction to the leuco-form. These findings are critically important for optimizing the parameters of systemic PDT using MB.

The study was funded by a grant from the Russian Science Foundation (project N 22-72-10117).

REFERENCES

- Foote C. S. Definition of type I and type II photosensitized oxidation, *Photochemistry and Photobiology*, 1991, vol. 54(5), pp. 659–659. doi: 10.1111/j.1751-1097.1991.tb02071.x.
- Baptista M. S., Cadet J., Di Mascio P. et al. Type I and Type II Photosen-sitized Oxidation Reactions: Guidelines and Mechanistic Pathways, Photochemistry and Photobiology, 2017, vol. 93(4), pp. 912–919. doi: 10.1111/php.12716.
- Li X., Kwon N., Guo T. et al. Innovative Strategies for Hypoxic-Tumor Photodynamic Therapy, *Angewandte Chemie International Edition*, 2018, vol. 57(36), pp. 11522–11531. doi: 10.1002/anie.201805138.
- Zhao X., Liu J., Fan J. et al. Recent progress in photosensitizers for overcoming the challenges of photodynamic therapy: from molecular design to application, *Chemical Society Reviews*, 2021, vol. 50(6), pp. 4185-4219. doi: 10.1039/D0CS00173B.
- Xu J., Bonneviot L., Guari Y. et al. Matrix Effect on Singlet Oxygen Gen-
- retain Using Methylene Blue as Photosensitizer, *Inorganics*, 2024, vol. 12(6), pp. 155. doi: 10.3390/inorganics12060155. Lucky S. S., Soo K. C., Zhang Y. Nanoparticles in Photodynamic Therapy, *Chemical Reviews*, 2015, vol. 115(4), pp. 1990–2042. doi: 10.1021/cr5004198.
- Filonenko E. V. Clinical implementation and scientific development of photodynamic therapy in Russia in 2010-2020, Biomedical Photonics,
- 2022, vol. 10(4), pp. 4–22. doi: 10.24931/2413-9432-2021-9-4-4-22. Semyonov D. Yu., Vasil'ev Yu. L., Dydykin S. S. et al. Antimicrobial and antimycotic photodynamic therapy (review of literature), *Biomedical Photonics*, 2021, vol. 10(1), pp. 25–31. doi: 10.24931/2413-9432-2021-
- Trushina O. I., Filonenko E. V., Novikova E. G. et al. Photodynamic therapy in the prevention of HPV-induced recurrences of precancer and initial cancer of the cervix, *Biomedical Photonics*, 2024, vol. 13(3), pp. 42–46. doi: 10.24931/241-9432-2024-13-3-42-46.
- Tseimakh A. E., Mitshenko A. N., Kurtukov V. A. et al. Effectiveness of palliative photodynamic therapy for unresectable biliary cancer. Systematic review and meta-analysis, *Biomedical Photonics*, 2024, vol. 13(2), pp. 34–42. doi: 10.24931/2413-9432-2024-13-2-
- Shanazarov N. A., Zinchenko S. V., Kisikova S. D. et al. Photodynamic therapy in the treatment of HPV-associated cervical cancer: mechanisms, challenges and future prospects, *Biomedical Photonics*, 2024, vol. 13(1), pp. 47–55. doi: 10.24931/2413-9432-2023-13-1-47-55. Panaseykin Y. A., Kapinus V. N., Filonenko E. V. et al. Photodynamic therapy in treatment of squamous cell carcinoma of oral cavity with
- chlorine e6 photosensitizer with long-term follow up, Biomedical Photonics, 2024, vol. 13(1), pp. 28-38. doi: 10.24931/2413-9432-2023-13-1-28-38.

ЛИТЕРАТУРА

- Foote C.S. Definition of type I and type II photosensitized oxidation // Photochemistry and photobiology. 1991. Vol. 54(5). P. 659-659. doi: 10.1111/j.1751-1097.1991.tb02071.x.
- Baptista M.S., Cadet J., Di Mascio Р. и др. Type I and type II photosensitized oxidation reactions: guidelines and mechanistic pathways // Photochemistry and photobiology. – 2017. – Vol. 93(4). – P. 912-919. doi: 10.1111/ php. 12716. Li X., Kwon N., Guo Т. и др. Innovative strategies for hypoxic-tumor pho-
- todynamic therapy // Angewandte chemie international edition. 2018. Vol. 57(36). P. 11522-11531. doi: 10.1002/ anie.201805138.
- Zhao X., liu J., Fan J. и др. Recent progress in photosensitizers for overcoming the challenges of photodynamic therapy: from molecular design to application // Chemical society reviews. – 2021. – Vol. 50 (6). – P. 4185-4219. doi: 10.1039/d0cs00173b.
- Xu J., Bonneviot L., Guari Y. и др. Matrix effect on singlet oxygen generation using methylene blue as photosensitizer // Inorganics. – 2024. – Vol. 12 (6). – P. 155. doi: 10.3390/inorganics12060155.
- Lucky S.S., Soo K.C., Zhang Y. Nanoparticles in photodynamic therapy // Chemical reviews. 2015. Vol. 115 (4). P. 1990-2042. doi: 10.1021/
- Филоненко Е.В. Клиническое внедрение и научное развитие фото-динамической терапии в России в 2010-2020 гг. // Biomedical Photonics. – 2021. – T. 10, № 4. – C. 4-22. doi: 10.24931/2413-9432-2021-9-4-4-22
- Семенов Д.Ю., Васильев Ю.Л., Дыдыкин С.С. и др. Антимикробная и антимикотическая фотодинамическая терапия (обзор литературы)// Biomedical Photonics. - 2021. - T. 10, №1. - C. 25-31. doi: 10.24931/2413-9432-2021-10-1-25-31. Трушина О.И., Филоненко Е.В., Новикова Е.Г. и др. Фотодинамическая
- терапия в профилактике ВТЧ- индуцированных рецидивов предра-ка и начального рака шейки матки // Biomedical Photonics. 2024. Т. 3, № 3. - C. 42-46. doi: 10.24931/241-9432-2024-13-3-42-46.
- Цеймах А.Е., Мищенко А.Н., Куртуков В.А. и др. Эффективность паллиативной фотодинамической терапии нерезектабельных злокачественных новообразований желчевыводящей системы. Систематический обзор и метаанализ // Biomedical Photonics. – 2024. – Т. 13, № 2. – C. 34-42. doi: 10.24931/2413-9432-2024-13-2-34-42.
- Шаназаров Н.А., Зинченко С.В., Кисикова С.Д. и др. Фотодинамическая терапия в лечении ВПЧ-ассоциированного рака шейки матки: механизмы, проблемы и перспективы на будущее // Biomedical Photonics. - 2024. - T. 13, № 1. - C. 47-55. doi: 10.24931/2413-9432-2023-13--47-55
- Панасейкин Ю.А., Капинус В.Н., Филоненко Е.В. и др. Результаты лечения больных раком полости рта при помощи фотодинамической терапии с фотосенсибилизатором на основе хлорина еб // Biomedi-

- Taldaev A., Terekhov R., Nikitin I. et al. Methylene blue in anticancer photodynamic therapy: systematic review of preclinical studies, Frontiers in Pharmacology, 2023, vol. 14, pp. 1264961. doi: 10.3389/ februages 1264961. fphar.2023.1264961.
- DeRosa M. Photosensitized singlet oxygen and its applications, *Coordination Chemistry Reviews*, 2002, vol. 233–234, pp. 351–371. doi: 10.1016/S0010-8545(02)00034-6.
 Redmond R. W., Gamlin J. N. A compilation of singlet oxygen yields from biologically relevant molecules, *Photochemistry and Photobiology*,
- 1999, vol. 70(4), pp. 391–475. doi: 10.1111/j.1751-1097.1999.tb08240.x. Tardivo J. P., Del Giglio A., De Oliveira C. S. et al. Methylene blue in photodynamic therapy: From basic mechanisms to clinical applications, *Photodiagnosis and Photodynamic Therapy*, 2005, vol. 2(3), pp. 175–191. doi: 10.1016/S1572-1000(05)00097-9.
- Medhi D., Hazarika S. Formation of dimer and higher aggregates of methylene blue in alcohol, Spectrochimica Acta Part A: Molecular and Biomólecular Spectroscopy, 2025, vol. 329, pp. 125490. doi: 10.1016/j.
- saa.2024.125490. Junqueira H. C., Severino D., Dias L. G. et al. Modulation of methylene
- Junqueira H. C., Severino D., Dias L. G. et al. Modulation of methylene blue photochemical properties based on adsorption at aqueous micelle interfaces, *Physical Chemistry Chemical Physics*, 2002, vol. 4(11), pp. 2320–2328. doi: 10.1039/b109753a.

 Severino D., Junqueira H. C., Gugliotti M. et al. Influence of negatively charged interfaces on the ground and excited state properties of methylene blue, *Photochemistry and Photobiology*, 2003, vol. 77(5), pp. 459–468. doi: 10.1562/0031-8655(2003)0772.0.co;2.
- Ball D. J., Luo Y., Kessel D. et al. The induction of apoptosis by a positively charged methylene blue derivative, *Journal of Photochemistry* and *Photobiology B:Biology*, 1998, vol. 42(2), pp. 159–163. doi: 10.1016/S1011-1344(98)00061-X.
- Curry S. Methemoglobinemia, Annals of Emergency Medicine, 1982, vol. 11(4), pp. 214–221. doi: 10.1016/S0196-0644(82)80502-7. Sass M. D., Caruso C. J., Axelrod D. R. Accumulation of methylene blue
- by metabolizing erythrocytes, *The Journal of Laboratory and Clinical Medicine*, 1967, vol. 69(3), pp. 447–455.

 Sakai H., Leong C. Prolonged functional life span of artificial red cells in blood circulation by repeated methylene blue injections, *Artificial Communications*, *Artificial Communications*,
- Cells, Nanomedicine, and Biotechnology, 2019, vol. 47(1), pp. 3123–3128. doi: 10.1080/21691401.2019.1645157.
 Sakai H., Li B., Lim W. L. et al. Red Blood Cells Donate Electrons to Methylene Blue Mediated Chemical Reduction of Methemoglobin Com-

- ylene Blue Mediated Chemical Reduction of Methemoglobin Compartmentalized in Liposomes in Blood, *Bioconjugate Chemistry*, 2014, vol. 25(7), pp. 1301–1310. doi: 10.1021/bc500153x.

 May J. M., Qu Z., Cobb C. E. Reduction and uptake of methylene blue by human erythrocytes, *American Journal of Physiology-Cell Physiology*, 2004, vol. 286(6), pp. C1390–C1398. doi: 10.1152/ajpcell.0051.2.2003.

 McDonagh E. M., Bautista J. M., Youngster I. et al. PharmGKB summary: methylene blue pathway, *Pharmacogenetics and Genomics*, 2013, vol. 23(9), pp. 498–508. doi: 10.1097/FPC.0b013e32836498f4.

 Harrop Geo. A., Barron E. S. G. STUDIES ON BLOOD CELL METABOLISM, *Journal of Experimental Medicine*, 1928, vol. 48(2), pp. 207–223. doi: 10.1097/FPC.0b013e328364987.
- Journal of Experimental Medicine, 1928, vol. 48(2), pp. 207–223. doi: 10.1084/jem.48.2.207.
- Pominova D., Ryabova A., Skobeltsin A. et al. The use of methylene blue to control the tumor oxygenation level, *Photodiagnosis and Photodynamic Therapy*, 2024, vol. 46, pp. 104047. doi: 10.1016/j.pdpdt.2024.104047.
- Pominova D. V., Ryabova A. V., Skobeltsin A. S. et al. Spectroscopic Study of Methylene Blue Interaction with Coenzymes and Its Effect on Tumor Metabolism, *Sovremennye tehnologii v medicine*, 2025, vol. 17(1), pp. 18. doi: 10.17691/stm2025.17.1.02.
- Ryabova A. V., Stratonnikov A. A., Loshchenov V. B. Laser spectroscopy technique for estimating the efficiency of photosensitisers in biological media, *Quantum Electronics*, 2006, vol. 36(6), pp. 562–568. doi: 10.1070/QE2006v036n06ABEH013291.
- Stratonnikov A. A., Loschenov V. B. Evaluation of blood oxygen saturation in vivo from diffuse reflectance spectra, *Journal of Biomedical*
- *Optics*, 2001, vol. 6(4), pp. 457. doi: 10.1117/1.1411979. Pominova D. V., Ryabova A. V., Romanishkin I. D. et al. Spectroscopic study of methylene blue photophysical properties in biological media, *Biomedical Photonics*, 2023, vol. 12(2), pp. 34–47. doi: 10.24931/2413-9432-2023- 12-2-34-47.
- Kalyanaraman B., Darley-Usmar V., Davies K. J. A. et al. Measuring reactive oxygen and nitrogen species with fluorescent probes: challenges and limitations, *Free Radical Biology and Medicine*, 2012, vol. 52(1), pp. 1–6. doi: 10.1016/j.freeradbiomed.2011.09.030.

 Marques S., Magalhães L., Tóth I. et al. Insights on Antioxidant Assays for Biological Samples Based on the Reduction of Copper Complex-
- -The Importance of Analytical Conditions, International Journal of Molecular Sciences, 2014, vol. 15(7), pp. 11387-11402. doi: 10.3390/ ijms150711387. George A., Pushkaran S., Li L. et al. Altered phosphorylation of cyto-
- George A., Pushkaran S., Li L. et al. Altered phosphorylation of cytoskeleton proteins in sickle red blood cells: The role of protein kinase C, Rac GTPases, and reactive oxygen species, *Blood Cells, Molecules, and Diseases*, 2010, vol. 45(1), pp. 41–45. doi: 10.1016/j.bcmd.2010.02.006. Gomes A., Fernandes E., Lima J. L. F. C. Fluorescence probes used for detection of reactive oxygen species, *Journal of Biochemical and Biophysical Methods*, 2005, vol. 65(2–3), pp. 45–80. doi: 10.1016/j.ibbm.2015.10.003.
- jbbm.2005.10.003.

- cal Photonics. 2024. T. 13, № 1. C. 28-38. doi: 10.24931/2413-9432-2023-13-1-28-38.
- Taldaev A., Terekhov R., Nikitin I. и др. Methylene blue in anticancer photodynamic therapy: systematic review of preclinical studies // Frontiers in pharmacology. – 2023. – Vol. 14. – P. 1264961. doi: 10.3389/ fphar.2023.1264961.
- DeRosa M. Photosensitized singlet oxygen and its applications // Coordination chemistry reviews. 2002. Vol. 23 (4). P. 351-371. doi: 10.1016/s0010-8545(02)00034-6.
- Redmond R.W., Gamlin J.N. A compilation of singlet oxygen yields from
- hedifiolid K.W., Garnilli J.K. A Compilation of singlet oxyget yields from biologically relevant molecules // Photochemistry and photobiology. 1999. Vol. 70(4). P. 391-475. doi: 10.1111/j.1751-1097.1999.tb08240.x. Tardivo J.P., Del Giglio A., De Oliveira C.S. и др. Methylene blue in photodynamic therapy: from basic mechanisms to clinical applications // Photodiagnosis and photodynamic therapy. 2005. Vol. 2(3). P. 175–191. doi: 10.1016/s1572-1000(05)00097-9.
- Medhi D., Hazarika S. Formation of dimer and higher aggregates of methylene blue in alcohol // Spectrochimica acta part a: molecular and biomolecular spectroscopy. 2025. Vol. 329. P. 125490. doi: 10.1016/j. saa.2024.125490.
- Junqueira H.C., Severino D., Dias L.G. и др. Modulation of methylene blue photochemical properties based on adsorption at aqueous micelle interfaces // Physical chemistry chemical physics. – 2002. – Vol. 4 (11). – P. 2320-
- 2328. doi: 10.1039/b109753a. Severino D., Junqueira H.C., Gugliotti M. и др. Influence of negatively charged interfaces on the ground and excited state properties of methy-
- charged interfaces on the ground and excited state properties of methylene blue // Photochemistry and photobiology. 2003. Vol.77(5). P. 459-468. doi: 10.1562/0031-8655(2003)0772.0.co;2.
 Ball DJ., Luo Y., Kessel D. и др. The induction of apoptosis by a positively charged methylene blue derivative // Journal of photochemistry and photobiology b: biology. 1998. Vol. 42 (2). P. 159-163. doi: 10.1016/s1011-1344(98)00061-x.
- Curry S. Methemoglobinemia // Annals of emergency medicine. 1982. Vol. 11(4), P. 214-221. doi: 10.1016/s0196-0644(82)80502-7.

 Sass M.D., Caruso C.J., Axelrod D.R. Accumulation of methylene blue by metabolizing erythrocytes // The journal of laboratory and clinical medicine. 1967. Vol. 69 (3). P. 447-455.
- Sakai H., Leong C. Prolonged Functional life span of artificial red cells in blood circulation by repeated methylene blue injections // Artificial cells, nanomedicine, and biotechnology. – 2019. – Vol. 47(1). – P. 3123-3128. doi:10.1080/21691401.2019.1645157.
- Sakai H., Li B., Lim W. L. и др. Red blood cells donate electrons to methylene blue mediated chemical reduction of methemoglobin compartmentalized in liposomes in blood // Bioconjugate chemistry. - 2014. - Vol. 25 (7). – P. 1301-1310. doi: 10.1021/bc500153x.
- May J.M., Qu Z., Cobb C.E. Reduction and uptake of methylene blue by human erythrocytes // American journal of physiology-cell physiology. 2004. Vol. 286 (6). P. 1390-1398. doi: 10.1152/ajpcell.00512.2003.
- 2004. Vol. 286 (δ). P. 1390-1398. doi: 10.1152/ajpceli.00512.2005. McDonagh E. M., Bautista J. M., Youngster I. и др. Pharmgkb summary: methylene blue pathway // Pharmacogenetics and genomics. 2013. Vol. 23(9). P. 498-508. doi: 10.1097/fpc.0b013e32836498f4. Harrop Geo. A., Barron E. S. G. Studies on blood cell metabolism // Journal of experimental medicine. 1928. Vol. 48 (2). P. 207-223. doi: 10.1084/
- jem.48.2.207
- Pominova D., Ryabova A., Skobeltsin A. и др. The use of methylene blue to control the tumor oxygenation level // Photodiagnosis and photodynamic therapy. 2024. Vol. 46. P. 104047. doi: 10.1016/j. pdndt 2024 104047
- Pominova D.V., Ryabova A.V., Skobeltsin A.S. и др. Spectroscopic study of methylene blue interaction with coenzymes and its effect on tumor metabolism // Sovremennye tehnologii v medicine. – 2025. – Vol. 17(1). – P.
- табовіят // sovernemy ternnologii v medicine. 2023. vol. 17(1). Р. 18. doi: 10.17691/stm2025.17.1.02. Рябова А.В., Стратонников А.А., Лощенов В. Б. Лазерно-спектроскопический метод оценки эффективности фотосенсибилизаторов в биологических средах // Квантовая электроника. 2006. Т. 36, № 6. C. 562-568. doi: 10.1070/ge2006v036n06abeh013291.
- Stratonnikov A.A., Loschenov V.B. Evaluation of blood oxygen saturation in vivo from diffuse reflectance spectra // Journal of biomedical optics. – 2001. – Vol. 6 (4). – Р. 457. doi: 10.1117/1.1411979. Поминова Д.В., Рябова А.В., Романишкин И.Д. и др. Спектроскопиче-
- ское исследование фотофизических свойств метиленового синего в биологических средах // Biomedical Photonics. 2023. Т. 12, № 2. С.
- 34-47. https://doi.org/10.24931/2413-9432-2023-12-2-34-47. Kalyanaraman B., Darley-Usmar V., Davies K.J.A. и др. Measuring reactive oxygen and nitrogen species with fluorescent probes: challenges and limitations // Free radical biology and medicine. 2012. Vol. 52(1). Р. 1-6. doi: 10.1016/j.freeradbiomed.2011.09.030.
- Marques S., Magálhães L., Tóth I. и др. Insights on antioxidant assays for
- Marques S., Magalhães L., Tóth I. и др. Insights on antioxidant assays for biological samples based on the reduction of copper complexes the importance of analytical conditions // International journal of molecular sciences. 2014. Vol. 15(7). P. 11387–11402. doi: 10.3390/ijms150711387. George A., Pushkaran S., Li L. и др. Altered phosphorylation of cytoskeleton proteins in sickle red blood cells: the role of protein kinase c, rac gtpases, and reactive oxygen species // Blood cells, molecules, and diseases. 2010. Vol. 45 (1). P. 41-45. doi: 10.1016/j. bcmd.2010.02.006. Gomes A., Fernandes E., Lima J.L.F.C. Fluorescence probes used for detection of reactive oxygen species // Journal of biochemical and biophysical methods. 2005. Vol. 65(2-3). P.45-80. doi: 10.1016/j.jbbm.2005.10.003.